

# Measuring Parton Energy Loss at RHIC compared to LHC

M. J. Tannenbaum<sup>‡</sup>, PHENIX Collaboration

Physics Department, Brookhaven National Laboratory, Upton, NY 11973-5000, USA

E-mail: mjt@bnl.gov

**Abstract.** The method of measuring  $\hat{x}_h = \hat{p}_{T_a}/\hat{p}_{T_t}$ , the ratio of the away-parton transverse momentum,  $\hat{p}_{T_a}$ , to the trigger-parton transverse momentum,  $\hat{p}_{T_t}$ , using two-particle correlations at RHIC, will be reviewed. This measurement is simply related to the two new variables introduced at LHC for the di-jet fractional transverse momentum imbalance: ATLAS  $A_J = (\hat{p}_{T_t} - \hat{p}_{T_a})/(\hat{p}_{T_t} + \hat{p}_{T_a}) = (1 - \hat{x}_h)/(1 + \hat{x}_h)$ ; and CMS  $\langle (\hat{p}_{T_t} - \hat{p}_{T_a})/\hat{p}_{T_t} \rangle = \langle 1 - \hat{x}_h \rangle$ . Results from two-particle correlations at RHIC for  $\hat{x}_h$  in p-p and A+A collisions will be reviewed and new results will be presented and compared to LHC results. The importance of comparing any effect in A+A collisions to the same effect in p-p collisions will be illustrated and emphasized.

## 1. Introduction

In 1998, at the QCD workshop in Paris, Rolf Baier asked me whether jets could be measured in Au+Au collisions because he had a prediction of a QCD medium-effect (energy loss via soft gluon radiation induced by multiple scattering [1] on color-charged partons traversing a hot-dense-medium composed of screened color-charges [2]). I told him [3] that there was a general consensus [4] that for Au+Au central collisions at  $\sqrt{s_{NN}} = 200$  GeV, leading particles are the only way to study jets, because in one unit of the nominal jet-finding cone,  $\Delta r = \sqrt{(\Delta\eta)^2 + (\Delta\phi)^2}$ , there is an estimated  $\pi\Delta r^2 \times \frac{1}{2\pi} \frac{dE_T}{d\eta} \sim 375$  GeV of energy (!) The good news was that hard-scattering in p-p collisions was originally observed by the method of leading particles and that these techniques could be used to study hard-scattering and jets in Au+Au collisions [5].

## 2. Hard scattering via single particle inclusive and two-particle correlation measurements

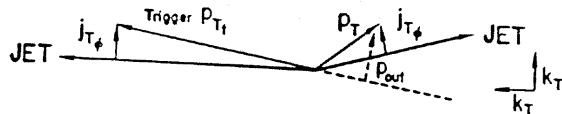
Single particle inclusive and two-particle correlation measurements of hard-scattering have provided a wealth of discoveries at RHIC. Due to the steeply falling power-law invariant transverse momentum spectrum of the scattered parton,  $\hat{p}_{T_t}^{-n}$ , the inclusive single particle (e.g.  $\pi^0$ )  $p_{T_t}$  spectrum from jet fragmentation is dominated by fragments

<sup>‡</sup> Supported by the U.S. Department of Energy, Contract No. DE-AC02-98CH1-886.

with large  $z_{\text{trig}}$ , where  $z_{\text{trig}} = p_{T_t}/\hat{p}_{T_t}$  is the fragmentation variable, and exponential fragmentation  $D_q^{\pi^0}(z) \sim e^{-bz}$  is assumed. This gives rise to several effects which allow precision measurements of hard scattering to be made using single inclusive particle spectra and two particle correlations [6, 7].

The prevailing opinion from the 1970's until quite recently was that although the inclusive single particle (e.g.  $\pi^0$ ) spectrum from jet fragmentation is dominated by trigger fragments with large  $\langle z_{\text{trig}} \rangle \sim 0.6 - 0.8$ , the away-jets should be unbiased and would measure the fragmentation function, once the correction is made for  $\langle z_{\text{trig}} \rangle$  and the fact that the jets don't exactly balance  $p_T$  due to the  $k_T$  smearing effect [8]. Two-particle correlations with trigger  $p_{T_t}$ , are analyzed in terms of the two variables:  $p_{\text{out}} = p_T \sin(\Delta\phi)$ , the out-of-plane transverse momentum of an associated track with  $p_T$ ; and  $x_E$ , where:

$$x_E = \frac{-\vec{p}_T \cdot \vec{p}_{Tt}}{|p_{Tt}|^2} = \frac{-p_T \cos(\Delta\phi)}{p_{Tt}} \simeq \frac{z}{z_{\text{trig}}}$$



$z_{\text{trig}} \simeq p_{T_t}/p_{T_{\text{jet}}}$  is the fragmentation variable of the trigger jet, and  $z$  is the fragmentation variable of the away jet.

However, in 2006, it was found by explicit calculation that this is not true [9, 6, 7]. The shape of the  $p_{T_a}$  spectrum of fragments (from the away-side parton with  $\hat{p}_{T_a}$ ), given a trigger particle with  $p_{T_t}$  (from a trigger-side parton with  $\hat{p}_{T_t}$ ), is not sensitive to the shape of the fragmentation function ( $b$ ), but measures the ratio of  $\hat{p}_{T_a}$  of the away-parton to  $\hat{p}_{T_t}$  of the trigger-parton and depends only on the same power  $n$  as the invariant single particle spectrum:

$$\left. \frac{dP_{p_{T_a}}}{dx_E} \right|_{p_{T_t}} \approx \langle m \rangle (n-1) \frac{1}{\hat{x}_h} \frac{1}{(1 + \frac{x_E}{\hat{x}_h})^n} \quad (1)$$

This equation gives a simple relationship between the ratio,  $x_E \approx p_{T_a}/p_{T_t} \equiv z_T$ , of the transverse momenta of the away-side particle to the trigger particle, and the ratio of the transverse momenta of the away-jet to the trigger-jet,  $\hat{x}_h = \hat{p}_{T_a}/\hat{p}_{T_t}$ . The only dependence on the fragmentation function is in the mean multiplicity  $\langle m \rangle$  of jet fragments. This functional form was shown previously [9, 10] (and with the present data, see below) to describe the  $\pi^0$  triggered  $x_E$  distribution in p-p collisions and is based only on the following simplifying assumptions: the hadron fragment is assumed to be collinear with the parton direction; the underlying fragmentation functions ( $D(z)$ ) are assumed to be exponential; and for a given  $p_{T_t}$ ,  $\hat{x}_h$  is taken to be constant as a function of  $x_E$  over the range of interest. The key issue with Eq. 1 is that it is independent of the slope of an exponential fragmentation function, and only depends on the detected mean multiplicity  $\langle m \rangle$  of the jet, the power,  $n$ , of the inclusive  $p_{T_t}$  spectrum and the ratio of the away jet to the trigger jet transverse momenta,  $\hat{x}_h$ .

### 3. Fits to PHENIX $\pi^0$ -h correlations

The two-particle correlation distributions from  $\pi^0$  triggers in four intervals of  $p_{T_t}$ , 4-5, 5-7, 7-9 and 9-12 GeV/c, with charged hadrons in a fixed range of associated transverse

momenta,  $p_{T_a} \approx 0.7, 1.3, 2.3, 3.5, 5.8$  GeV/c were recently published by PHENIX [11] in terms of the ratio of A+A to p-p collisions,  $I_{AA}(p_{T_a})|_{p_{T_t}} = \frac{dP^{AA}/dp_{T_a}}{dP^{pp}/dp_{T_a}}|_{p_{T_t}}$  (see Fig. 1).

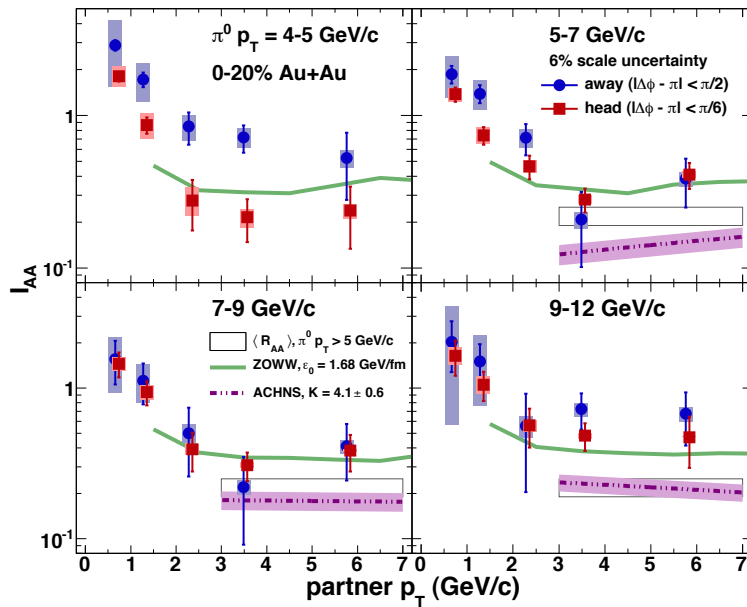


**Figure 1.** Away-side  $I_{AA}$  [11] for a narrow “head”  $|\Delta\phi - \pi| < \pi/6$  selection (solid squares) and the entire away-side,  $|\Delta\phi - \pi| < \pi/2$  (solid circles) as a function of partner momentum  $p_{T_a}$  for various trigger momenta  $p_{T_t}$ . Only the head region was used for the present analysis.

We now analyze these distributions separately for p-p and Au+Au collisions, with the statistical error and the larger of the  $\pm$  systematic errors of the data points added in quadrature. The p-p and Au+Au distributions in  $z_T = p_{T_a}/p_{T_t}$  were fit to the formula [9]:

$$\left. \frac{dP_\pi}{dz_T} \right|_{p_{T_t}} = N(n-1) \frac{1}{\hat{x}_h} \frac{1}{(1 + \frac{z_T}{\hat{x}_h})^n}, \quad (2)$$

with a fixed value of  $n = 8.10 (\pm 0.05)$  as previously determined [12], where  $n$  is the power-law of the inclusive  $\pi^0$  spectrum and is observed to be the same in p-p and Au+Au collisions in the  $p_{T_t}$  range of interest. The fitted value for  $N$  is the integral of the  $z_T$  distribution which equals  $\langle m \rangle$ , the mean multiplicity of the away jet in the PHENIX detector acceptance, and  $\hat{x}_h \equiv \hat{p}_{T_a}/\hat{p}_{T_t}$  is the ratio of the away jet to the trigger jet transverse momenta.

Fits were performed for the p-p spectra; and also for the Au+Au spectra at two centralities: 0-20% and 20-40% upper-percentiles. The parameters of the p-p distribution,  $\hat{x}_h^{pp}$  and  $N_{pp}$ , are determined by fits of Eq. 2 to the p-p data for the four intervals of  $p_{T_t}$ ; and the parameters  $\hat{x}_h^{AA}$  and  $N_{AA}$  are determined from the fits to the Au+Au distributions. The fits were performed only for the narrower “head” region,  $|\Delta\phi - \pi| < \pi/6$ . It should be noted that in Fig. 1, there is no difference in the results ( $I_{AA}$ ) for the full away side and the head region, for  $p_{T_t} \geq 7$  GeV/c, because the non-jet

background becomes sufficiently small so that the “shoulder” [13], now known to be due to a  $v_3$  background modulation [14] for which no correction has been applied in this data, contributes negligibly to the away-side yield.

#### 4. Results of the fits

Examples of the fits for  $7 < p_{T_t} < 9$  GeV/c for p-p collisions and Au+Au 0–20% and 20–60% are shown in Figs. 2a and b, respectively. The results for the fitted parameters

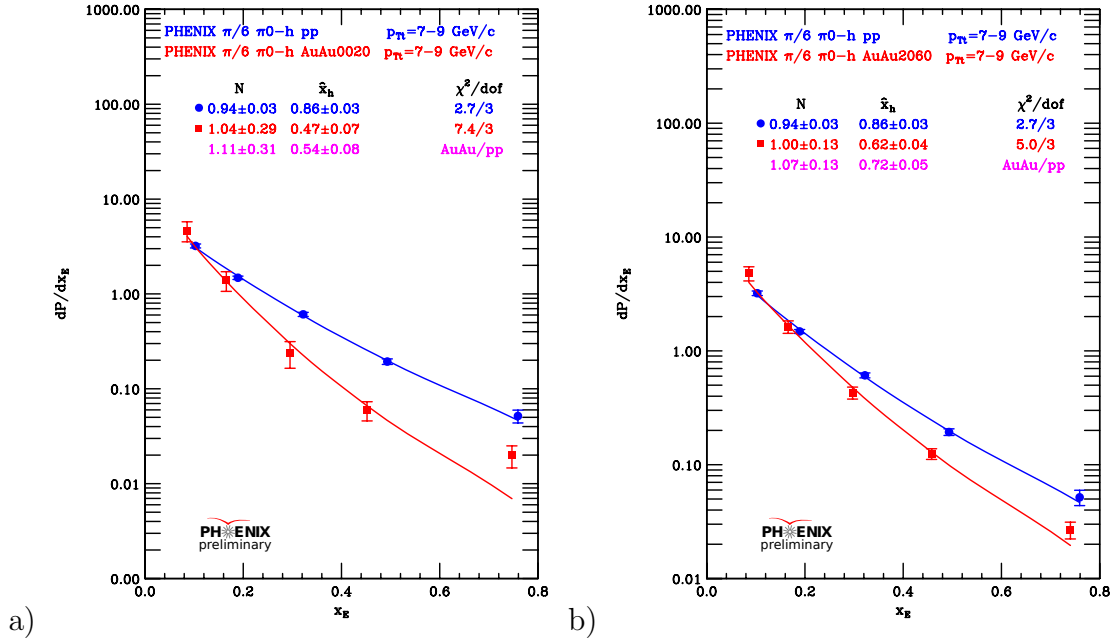


**Figure 2.** p-p (blue circles) and AuAu (red squares)  $z_T = p_{T_a} / \langle p_{T_t} \rangle$  distributions for  $p_{T_t} = 7 - 9$  GeV/c ( $\langle p_{T_t} \rangle = 7.71$  GeV/c), together with fits to Eq. 2 p-p (solid blue line), AuAu (solid red line) with parameters indicated: a) 00-20% centrality, b) 20–60% centrality. The ratios of the fitted parameters for AuAu/pp are also given.

are shown on the figures. In general the values of  $\hat{x}_h^{pp}$  do not equal 1 but range between  $0.8 < \hat{x}_h^{pp} < 1.0$  due to  $k_T$  smearing and the range of  $z_T$  covered. For the fixed range of associated  $p_{T_a}$  0.7 – 5.8 GeV/c, the lowest  $p_{T_t} = 4 - 5$  GeV/c trigger provides the most balanced same and away side jets, with  $\hat{x}_h \approx 1.0$ , while as  $p_{T_t}$  increases up to 9–12 GeV/c, for the fixed range of  $p_{T_a}$ , the jets become unbalanced towards the trigger side in p-p collisions due to  $k_T$  smearing. Thus, in the present data, the  $p_{T_t}$  and  $z_T$  ranges are identical for the p-p and Au+Au comparison. Furthermore, in order to take account of the imbalance ( $\hat{x}_h^{pp} < 1$ ) observed in the p-p data, the ratio  $\hat{x}_h^{AA} / \hat{x}_h^{pp}$  is taken as the measure of the energy of the away jet relative to the trigger jet in A+A compared to p-p collisions.

It is important to note that the away jet energy fraction in AuAu relative to p-p,  $\hat{x}_h^{AA} / \hat{x}_h^{pp} = 0.47/0.86 = 0.54 \pm 0.08$  in Fig. 2a, is significantly less than 1, indicating energy loss of the away jet in the medium. Also since the away-jet may suffer different

energy losses for a given trigger jet  $\hat{p}_{T_t}$  due to variations in the path-length through the medium,  $\hat{x}_h^{AA}$  should be understood as  $\langle \hat{x}_h^{AA} \rangle$ .

## 5. LHC Results

In very exciting first results from the LHC heavy ion program, ATLAS [15] observed dijet events in Pb+Pb central collisions at  $\sqrt{s_{NN}} = 2.76$  TeV with a large energy asymmetry which they characterized by a new quantity  $A_J = (1 - \hat{x}_h^{AA}) / (1 + \hat{x}_h^{AA})$ . Shortly thereafter, CMS [16] presented a plot of  $\langle 1 - p_{t,2}/p_{t,1} \rangle = 1 - \langle \hat{x}_h^{AA} \rangle$ , the fractional jet imbalance as a function of  $E_{T1}$  up to 200–220 GeV with a cut  $E_{T2} \geq 50$  GeV (Fig. 3). If there were no cuts on the p-p jets used in this measurement, then this variable should be identical to the one we call  $1 - \hat{x}_h^{AA}/\hat{x}_h^{pp}$ , the away-parton fractional energy loss (or imbalance) in A+A relative to p-p. However, due to the cut used in the CMS data, the sample of di-jets

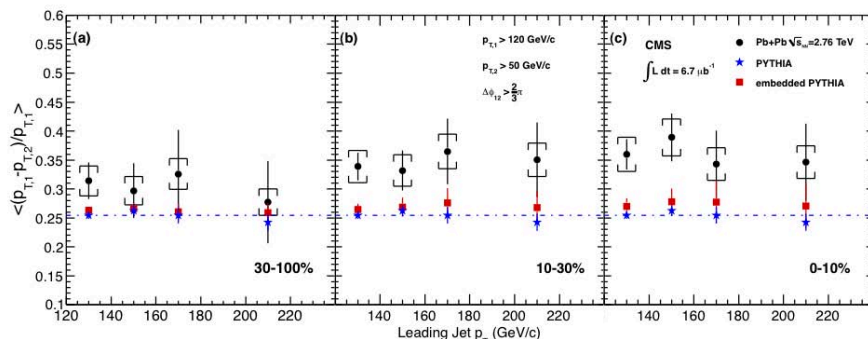


**Figure 3.** CMS [16] plot of  $\langle 1 - p_{t,2}/p_{t,1} \rangle$ , the fractional jet imbalance, as a function of  $p_{T,1}$  for 3 centralities in p-p and Pb+Pb collisions.

in p-p used to compare with A+A suffers from a large imbalance of 0.25, independent of  $E_{T1}$  (Fig. 3). We correct this by calculating  $\hat{x}_h^{AA}$  and  $\hat{x}_h^{pp}$  for CMS from their given values of  $1 - \hat{x}_h^{AA}$  and  $1 - \hat{x}_h^{pp}$  and then correcting to  $1 - \hat{x}_h^{AA}/\hat{x}_h^{pp}$ . For instance, in Fig. 3c for  $E_{T1} = 130$  GeV,  $\langle 1 - \hat{x}_h^{pp} \rangle = 0.255$  (i.e.  $\langle \hat{x}_h^{pp} \rangle = 0.745$ ), while  $\langle 1 - \hat{x}_h^{AA} \rangle = 0.36$  (i.e.  $\langle \hat{x}_h^{AA} \rangle = 0.64$ ), so that  $1 - \langle \hat{x}_h^{AA} \rangle / \langle \hat{x}_h^{pp} \rangle = 1 - (0.64/0.745) = 0.141$ .

The corrected points are shown together with the PHENIX data for  $1 - \hat{x}_h^{AA}/\hat{x}_h^{pp}$ , which we denote for simplicity  $\langle 1 - \hat{x}_h \rangle$ , the observed fractional jet imbalance in A+A relative to p-p (Fig. 4). Of course the CMS result is directly measured with jets, while the PHENIX value is deduced from the fragments of the dijets using a few simple assumptions, as noted above. The PHENIX data are plotted at the presumed mean trigger parton transverse momentum  $\langle \hat{p}_{T_t} \rangle = p_{T_t} / \langle z_{\text{trig}} \rangle$ , where the average fragmentation fraction of the trigger particle,  $\langle z_{\text{trig}} \rangle \approx 0.7$ , was derived in Ref. [9]. There is a clear difference in fractional jet imbalance in going from RHIC to LHC in central collisions—the jet-imbalance or fractional energy loss is much smaller at LHC. This is different from the first impression [15]. Also at RHIC, there is less fractional energy loss or jet imbalance in less central collisions.

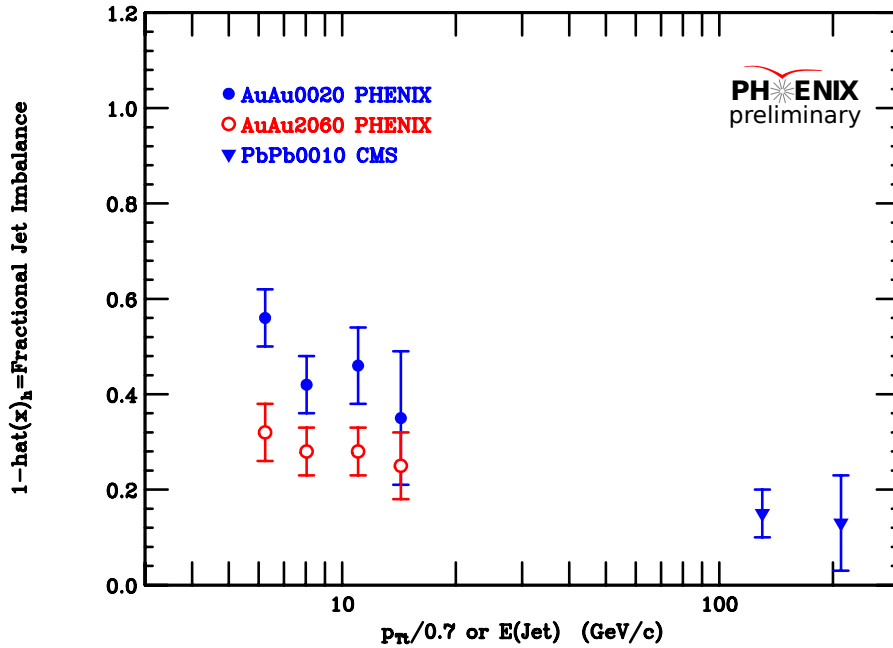


**Figure 4.** Away-jet fractional imbalance or energy loss in A+A relative to p-p,  $1 - \hat{x}_h$ , as a function of  $p_{T_t}/0.7$  for PHENIX and  $E(\text{Jet})$  for CMS, with centralities indicated.

The large difference in fractional jet imbalance between RHIC and LHC c.m. energies could be due to the difference in jet  $\hat{p}_{T_t}$  between RHIC ( $\sim 20$  GeV/c) and LHC ( $\sim 200$  GeV/c), the difference in  $n$  for the different  $\sqrt{s}$ , or to a difference in the properties of the medium. Future measurements will need to sort out these issues by extending both the RHIC and LHC measurements to overlapping regions of  $p_T$ .

## References

- [1] R. Baier, Yu. Dokshitzer, S. Peigné and D. Schiff, Phys. Lett. **B345**, 277–286 (1995).
- [2] R. Baier *QCD, Proc. IV Workshop-1998 (Paris)* Eds, H. M. Fried, B. Müller (World Scientific, Singapore, 1999) pp 272–279.
- [3] M. J. Tannenbaum *ibid.*, pp 280–285, pp 312–319.
- [4] e.g. see *Proc. Int'l Wks. Quark Gluon Plasma Signatures (Strasbourg)* Eds. V. Bernard, *et al.*, (Editions Frontieres, Gif-sur-Yvette, France, 1999).
- [5] M. J. Tannenbaum, Nucl. Phys. **A749**, 219c–228c (2005).
- [6] See Ref. [7] for a more thorough treatment with a full list of references.
- [7] M. J. Tannenbaum, PoS(CFRNC2006)001.
- [8] R. P. Feynman, R. D. Field and G. C. Fox, Nucl. Phys. **B128**, 1–65 (1977).
- [9] S. S. Adler, *et al.* PHENIX Collaboration, Phys. Rev. **D74**, 072002 (2006).
- [10] A. Adare, *et al.* PHENIX Collaboration, Phys. Rev. **D82**, 072001 (2010).
- [11] A. Adare, *et al.* PHENIX Collaboration, Phys. Rev. Lett. **104**, 252301 (2010).
- [12] A. Adare, *et al.* PHENIX Collaboration, Phys. Rev. Lett. **101**, 232301 (2008).
- [13] A. Adare, *et al.* PHENIX Collaboration, Phys. Rev. **C77**, 011901(R) (2008).
- [14] A. Adare, *et al.* PHENIX Collaboration, arXiv:1105.3928v1, submitted to Phys. Rev. Lett.
- [15] G. Aad, *et al.* (ATLAS Collaboration), Phys. Rev. Lett. **105**, 252303 (2010).
- [16] The CMS Collaboration, arXiv:1102.1957v2, submitted to Phys. Rev. C.